Laser parallel nanofabrication by single femtosecond pulse near-field ablation using photoresist masks

Florin Jipa,[1] Adrian Dinescu,[2] Mihaela Filipescu,[1] Iulia Anghel,[1] Marian Zamfirescu,[1,*] and Razvan Dabu[1,3]

[1]*National Institute for Laser, Plasma and Radiation Physics, Atomistilor 409, 077125 Măgurele, Romania*
[2]*National Institute for Microtechnology, Str. Erou Iancu Nicolae 126A, 077190 Bucharest, Romania*
[3]*National Institute for Nuclear Physics and Engineering, Reactorului 30, 077125 Magurele, Romania*
[*]*marian.zamfirescu@inflpr.ro*

Abstract: A new near-field processing method by femtosecond laser ablation using photoresist enhancing masks is numerically and experimentally investigated. Periodical structures with 2 μm pitch, 1 μm width and 300 nm height, created in polymethyl methacrylate photoresist by e-beam lithography, were used to intensify the incident laser radiation. The near-field distribution and the intensification factor of the optical radiation were computed using the Finite-Difference-Time-Domain numerical simulations. The pattern of the photoresist mask was imprinted on the surface of a silicon wafer. Using a single infrared femtosecond laser pulse, uniform and continuum grooves with the width in the range of 250 nm were obtained on large silicon surface.

OCIS codes: (220.4241) Nanostructure fabrication; (350.3390) Laser materials processing; (310.6628) Subwavelength structures, nanostructures.

References and links

1. A. Plech, P. Leiderer, and J. Boneberg, "Femtosecond laser near field ablation," Laser Photon. Rev. **5**(3), 435–451 (2009).
2. Z. B. Wang, N. Joseph, L. Li, and B. S. Luk'yanchuk, "A review of optical near-fields in particle/tip-assisted laser nanofabrication," Proc. Inst. Mech. Eng. Part C. **224**(5), 1113–1127 (2010).
3. A. Gorbunov and W. Pompe, "Thin Film Nanoprocessing by Laser/STM Combination," Phys. Status Solidi, A Appl. Res. **145**(2), 333–338 (1994).
4. K. Piglmayer, R. Denk, and D. Bäuerle, "Laser-induced surface patterning by means of microspheres," Appl. Phys. Lett. **80**(25), 4693–4695 (2002).
5. B. G. Prevo and O. D. Velev, "Controlled, Rapid Deposition of Structured Coatings from Micro- and Nanoparticle Suspensions," Langmuir **20**(6), 2099–2107 (2004).
6. R. Kunz, M. Rothschild, and M. Yeung, "Large-area patterning of ~50 nm structures on flexible substrates using near-field 193 nm radiation," J. Vac. Sci. Technol. B **21**(1), 78 (2003).
7. M. Ulmeanu, M. Zamfirescu, L. Rusen, C. Luculescu, A. Moldovan, A. Stratan, and R. Dabu, "Structuring by field enhancement of glass, Ag, Au, and Co thin films using short pulse laser ablation," J. Appl. Phys. **106**(11), 114908 (2009).
8. W. Cai and R. Piestun, "Patterning of silica microsphere monolayers with focused femtosecond laser pulses," Appl. Phys. Lett. **88**(11), 111112 (2006).
9. W. Guo, Z. Wang, L. Li, D. Whitehead, B. Luk'yanchuk, and Z. Liu, "Near-field laser parallel nanofabrication of arbitrary-shaped patterns," Appl. Phys. Lett. **90**(24), 243101 (2007).
10. E. Betzig, J. Trautman, R. Wolfe, E. Gyorgy, P. Finn, M. H. Kryder, and C. Chang, "Nearfield magnetooptics and high density data storage," Appl. Phys. Lett. **61**(2), 142–144 (1992).
11. R. Riehn, A. Charas, J. Morgado, and F. Cacialli, "Near-field optical lithography of a conjugated polymer," Appl. Phys. Lett. **82**(4), 526–528 (2003).
12. E. McLeod and C. B. Arnold, "Array-based optical nanolithography using optically trapped microlenses," Opt. Express **17**(5), 3640–3650 (2009).
13. S. Maruo, O. Nakamura, and S. Kawata, "Three-dimensional microfabrication with two-photon-absorbed photopolymerization," Opt. Lett. **22**(2), 132–134 (1997).

#200957 - $15.00 USD Received 7 Nov 2013; revised 21 Jan 2014; accepted 21 Jan 2014; published 5 Feb 2014

14. A. Taflove and S. Hagness Computational Electrodynamics, The Finite-Difference Time-Domain Method, (Artech House, Boston, 2005).
15. R. K. Harrison and A. Ben-Yakar, "Role of near-field enhancement in plasmonic laser nanoablation using gold nanorods on a silicon substrate: reply," Opt. Express **19**(7), 6179–6181 (2011).
16. S. Lecler, Y. Takakura, and P. Meyrueis, "Properties of a three-dimensional photonic jet," Opt. Lett. **30**(19), 2641–2643 (2005).
17. C. V. Shank, R. Yen, and C. Hirlimann, "Time-Resolved Reflectivity Measurements of Femtosecond-Optical-Pulse-Induced Phase Transitions in Silicon," Phys. Rev. Lett. **50**(6), 454–457 (1983).
18. D. Eversole, B. Luk'yanchuk, and A. Ben-yakar, "Plasmonic laser nanoablation of silicon by the scattering of femtosecond pulses near gold nanospheres," Appl. Phys., A Mater. Sci. Process. **89**(2), 283–291 (2007).
19. B. S. Luk'yanchuk, N. Arnold, S. M. Huang, Z. B. Wang, and M. H. Hong, "Three-dimensional effects in dry laser cleaning," Appl. Phys., A Mater. Sci. Process. **77**, 209–215 (2003).
20. L. Urech and T. Lippert, *Photochemistry and Photophysics of Polymer Materials*, (Wiley, 2010), Chap 14.

1. Introduction

The current trend towards the fabrication of sub-micrometer structures requires new methods and technologies for surface nano-patterning. In the last years, near-field laser ablation was intensively studied as efficient structuring method with spatial resolution much below the exposure wavelength [1,2]. Using the enhancement of the electro-magnetic field around micro-objects, the laser beam can be focused in tiny volumes below the diffraction limit. Then, by laser ablation, sub-wavelength surface structures can be obtained at the interface of the micro- and nano-particles with the surface to be processed [3,4]. Applying this effect to self-assembled colloidal particles [5], large areas can be processed using single laser pulses [6,7]. This method has the advantage of short processing time on large areas with typical features size on nanoscale range. The nanopatterns imprinted on the material surface are limited by the hexagonal arrangement of the monodispersed colloidal particles. Besides the geometrical limitations to hexagonal symmetry, the uniformity and orientation of the self-assembled monolayers of colloidal particles are hardly controlled on extended surfaces.

New methods for obtaining arbitrary shapes in the near-field exposure regime were recently proposed. The selective exposure of individual silica colloidal particle using focused lasers [8], the tuning of the angle of laser incidence for changing the position of the enhanced light spot underneath the colloidal particles [9], the near-field scanning optical microscope (NSOM) patterning [10,11] or the near-field nanopatterning using optical trapping of the microbeads [12] are some examples. However, such methods are not adapted for applications requiring a high throughput due to complex devices and/or slow processing time.

To improve the efficiency and versatility of the method, we propose to replace the usual self-arranged particles with engineered optical microstructures used as masks for optical enhancement. Such masks can be produced in photoresists materials by e-beam lithography approach, or by other lithographic method such as two-photon photopolymerization [13]. Then, employing the enhancement of the electro-magnetic field at the interface of the mask with the surface to be processed, any deterministic shape can be imprinted on materials surfaces by laser ablation in near-field regime.

In this paper a new processing method based on laser near-field enhancement underneath photoresist masks is presented. A transparent polymethyl methacrylate (PMMA) photoresist mask, created by e-beam lithography, was used as near-field intensifier for laser ablation. The theoretic near-field intensity distribution as well as the value of the enhancement factor produced by the mask is presented in the modeling section. The proposed method was experimentally tested by structuring a silicon material. The intensity of a single near infrared (NIR) femtosecond laser pulse was enhanced underneath the photoresist mask creating sub-wavelength structures on a silicon surface. The experimental results and theoretical simulations are correlated and discussed in the results section. The advantages of the proposed method are presented.

#200957 - $15.00 USD Received 7 Nov 2013; revised 21 Jan 2014; accepted 21 Jan 2014; published 5 Feb 2014

2. Modeling of the near-field intensity distribution

The proposed technique was theoretically investigated using a commercial software package, FULLWave 8.1 (RSoft Design Group), based on Finite-Difference-Time-Domain (FDTD) method [14]. In this algorithm the electromagnetic field propagating through the microstructured mask is computed by solving the Maxwell's curl equations as a function of discrete time and space. Then, the optical near-field intensity distribution and the optical enhancement factor produced by the designed mask are obtained. In the simulations, a spatially extended source at 775 nm wavelength with a constant intensity over the irradiated area was considered. The light is propagated through a transparent photoresist mask with refractive index 1.48. In the design, the mask was considered as a periodical rectangular grating with 2 μm period, 300 nm height, and 50% filling factor (1:1 ratio between air gaps and photoresist width). Different mask structures periods from 0.5 μm to 4 μm have been investigated. From the numerical studies it results that for 775 nm laser wavelength, the ideal rectangular structure with a period of 2 μm shows the most extended focal region, suitable for laser processing, less sensitive to the variation of the mask-substrate distance (*d*), or to the substrate planarity.

Under the experimental conditions, the mask profile was not perfectly rectangular. The field distribution and enhancement factor depend on the real shape of the intensifying micro-optics. For this reason, instead of using an ideal rectangular shaped-mask, the real profile was considered in the simulation, as measured by Atomic Force Microscopy (AFM), see section 3. By this approach, the theoretic enhancement factor, as well as the near-field distribution can be much better correlated with the real experimental conditions.

The representation of the near-field distribution can be done by the electric field intensity - $|E|^2$, or by the Poynting vector magnitude - $|S|$, depending on the wave approximation conditions [15]. Since the features of the polymerized mask are of the order of incident laser wavelength, the plane wave approximation is not valid in this case. Following the argumentation of previous works of R. K. Harrison et al. [15], for computing the near-field enhancement factor and for representation of the field distributions we used the Poynting vector magnitude for Z direction, $|S_z|$. The propagation of the laser wavelength (775 nm) through the photoresist mask was analyzed considering two situations: a) the polymer mask in free-space, in order to investigate the shape and the length of the high intensity region under the mask, the so called “photonic-jet” [16], and b) the mask placed in the proximity of a target with different air gaps. For the free-space case, the numerical simulation reveals a region were the field intensification is much extended in Z direction (about 4 μm) [Fig. 1(a)].

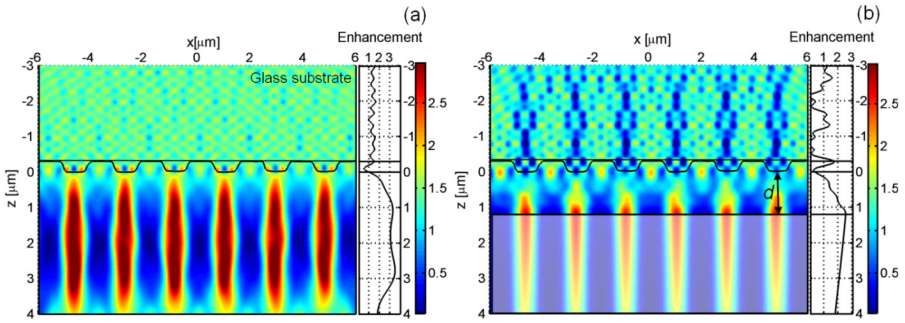

Fig. 1. Cross-section view of the Poynting vector magnitude $|S_z|$. (a) the photoresist mask in free-space. (b) for 1.2 μm gap between mask and the silicon wafer. The photoresist mask was centered at 0 position on the Z axis. The silicon wafer is placed at distance *d* from the mask. The insets on the right side of the images represent the intensity profiles taken in Z direction.

The distribution of the intensified optical field is uniform over a few micrometers distance. The maximum enhancement factor of more than 3 was obtained at distances *d* from

#200957 - $15.00 USD Received 7 Nov 2013; revised 21 Jan 2014; accepted 21 Jan 2014; published 5 Feb 2014

about 0.8 μm up to 3.2 μm away from the mask. Such extended focal region could be exploited for near-field laser nanofabrication. When a target is placed in the focal region at distance *d* from the mask, laser ablated nanostructures can be created. The effect of photonic-jet allows a small variation of the gap *d* without inducing an important shape change of the laser fabricated nano-patterns. When a material is placed in the vicinity of the mask some effects like optical cavity resonance could change the optical intensity distribution. For this reason, the simulations were also performed considering a silicon target placed at different positions from the photoresist mask.

In Fig. 1(b), a particular case is presented, where the value of *d* is 1.2 μm. The cross section profiles on both Z and X directions are shown. The right side inset of the picture represents the Z profile at the maximum value of the intensified optical field. The impact of different values for *d* on the intensification factor was also numerically investigated by FDTD. For the range of the investigated air gaps varying from 0 to 4 μm, the maximum intensification factor is obtained at the interface with the silicon target. In simulation, due to the optical penetration depth in Si of the photons at 775 nm wavelength, the optical beam seams to propagate over a distance of about 4-5 μm inside the material. However, in femtosecond pulses regime, the nonlinear absorption mechanism will have a strong effect on the propagation depth [17]. For values of *d* larger than 4 μm, the position of the maximum intensity remains in the region between the mask and the substrate. The results of the computed enhancement factor in function of the gap values are summarized in Fig. 2. A maximum intensification factor with a value of 2.6 was obtained for an air gap of $d = 1.2$ μm, as shown in Fig. 1(b).

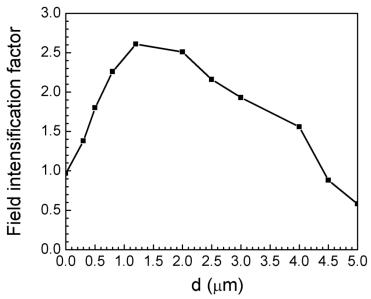

Fig. 2. Field intensification factor on silicon surface for different positions of target relative to photoresist mask.

In Fig. 2 it can be seen that the enhancement factor varies less than 10% relative to the maximum value of 2.6 when *d* varies from 1 μm to 2.5 μm, and less than 50% when *d* is varied from 0.3 to 4 μm. Since the variation of the *d* value will not give a steep variation of the enhancement factor, the distance between the mask and the substrate is not critical. Consequently, the planarity and gap control is not critical in the micrometer range permitting the laser intensification and laser ablation in near-field regime.

3. Experimental conditions

The ablation method based on optical near-field intensification using engineered photoresist masks was experimentally tested on a silicon surface. The mask was obtained by electron beam lithography in PMMA 950k A4 positive photoresist. Using the spin-coating method, a 300 nm thick layer was deposited on a 0.5 mm thick glass support previously cleaned using a standard cleaning procedure. The PMMA was backed 1 hour at 170 deg Celsius and subsequently covered with a conductive polymer (ESPACER 300) meant to dissipate the electric charge during the electron beam irradiation. A Raith e_Line, electron beam lithography workstation was used to create a pattern on the substrate. The designed mask consists in parallel lines with a period of 2 μm and a length of 300 μm. The pattern was

#200957 - $15.00 USD Received 7 Nov 2013; revised 21 Jan 2014; accepted 21 Jan 2014; published 5 Feb 2014

created in PMMA resist using 10kV accelerating voltage, 200 pA beam current, 10 mm working distance and 100 μC/cm^2 clearing dose. After exposure, the conductive polymer was removed by rinsing the sample in deionized water. The PMMA resist was developed for 2 min. at 20 deg. Celsius in a Methyl-Isobutyl-Ketone:Isopropyl alcohol (MIBK:IPA) mixture.

The mask was characterized by AFM [Fig. 3(a)]. For more accurate numerical results, the quasi rectangular profile [Fig. 3(d)] with round corners was used in the FDTD numerical simulation previously described. The fabricated mask was placed on the surface of a silicon wafer. A laser workstation coupled with a femtosecond laser system CPA 2101 (Clark-MXR) was used to irradiate the photoresist mask. The laser delivers pulses at 2 kHz in burst mode or single pulse regime, with 200 fs pulse duration at 775 nm wavelength and as much as 0.7 mJ pulse energy. The mask was irradiated by a single laser pulse. The desired laser fluence on large area was reached by slightly defocusing the laser beam. The focusing lens has 75 mm focal length. The sample was placed 10 mm in front of the focus plane. At this distance, the laser beam has a diameter of about 530 μm, measured at 1/e^2. Due to the Gaussian distribution of the energy in this plane the fluence can be considered quasi-constant over an exposed area with ~100 μm diameter. In this area, the laser fluence of 0.14 J/cm^2 used to irradiate the mask varies less than 10% and the resulted structures are uniform.

4. Results and discussion

The optical near-field intensification effect was investigated experimentally by varying the laser fluence bellow the ablation threshold of the silicon, 0.2 J/cm^2, measured for single femtosecond pulse irradiation regime [18]. When the sample was irradiated below this threshold without using the intensification mask, the silicon surface remains unaffected, in agreement with the threshold values from literature. If the mask is used, for the same laser fluence of 0.2 J/cm^2 and below, the surface is nanostructured, as shown in the Fig. 3(b) and Fig. 3(c). Uniform and continuum parallel groove structures with sub wavelength dimensions were created on silicon surface.

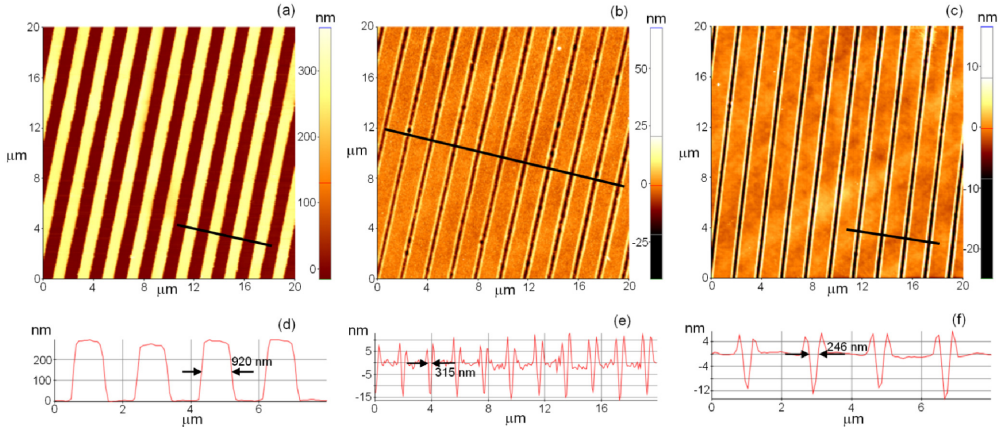

Fig. 3. The AFM image of the PMMA photoresist mask (a) and of the imprinted pattern at two locations inside the area of quasi-constant intensity: in the center of the exposed zone (b) and at approximately 50 μm far from center, (c). The AFM profiles of the mask (d) and the produced pattern (e) and respectively (f).

Below the intensity of 0.1 J/cm^2 the sample surface remains non-structured, even in near-field ablation regime. This information was correlated with the FDTD estimation of the intensification factor. In the literature, a large debate exists around the subject of metrics for evaluating the energy absorption for laser ablation in optical near-field regime. The intensity can be defined as $I = |E|^2$, or as $I = \boldsymbol{S}_z$, where $\boldsymbol{S}_z$ is the z-component of the Poynting vector. For the case of spherical particles both evaluations of the enhancement give similar results.

#200957 - $15.00 USD Received 7 Nov 2013; revised 21 Jan 2014; accepted 21 Jan 2014; published 5 Feb 2014

However, in the case of our polymer mask, due to the broken symmetry, the numerical simulation gives an evaluation of the E-field enhancement of about 6, much higher than the Poynting vector enhancement of 2.6. Since for near-field regime, at intensities lower than 0.1 J/cm^2 no structuring is obtained, we can estimate an experimental enhancement of about 2, closer to the value given by the Poynting vector evaluation, sustaining the hypothesis of Luk'yanchuk *et al.* [19] that the *z* component of the Poynting vector describes better the enhanced near-field intensity distribution.

In the experimental setup, the photoresist mask was placed directly on the silicon wafer without any additional pressure. With this configuration, the value of *d* cannot be precisely controlled at sub-micrometer level. Normally, for usual near-field laser processing using self-assembled particle arrays, a variation of the distance *d* between the particles and the surface might induce non-uniform patterns on the target surface. This possible drawback is eliminated in the case of the fabricated mask due to the extended focal region which compensates the small gap variations [Fig. 1]. Due to the extended focal region, it is not compulsory to have the mask in direct contact with the surface of the material. This assumption was investigated by analyzing the uniformity of the structures in the region of quasi-constant intensity. Several areas were scanned by the AFM tip around the central region were the laser intensity varies less than 10%. The averaged values of the grooves widths and deeps were compared. Two images, one in the center of the area and the other placed at about 50 μm far are reported in the Fig. 3(b) and Fig. 3(c), respectively. The grooves in the center of the irradiated area are 16.8 ± 3.4 nm deep and 315 ± 38 nm large [Fig. 3(b)]. At the second location, were the intensity is estimated to decrease at 90% from maximum, the grooves are 13.87 ± 2.05 nm deep and 246 ± 18 nm large [Fig. 3(c)]. Inside the processed area of ~100 μm diameter, a variation of ~20% was measured on grooves averaged dimensions from the 20 μm x 20 μm AFM investigated areas. An extended imprinted area could be obtained if a "flat-top" beam profile would be used.

Other advantage of this method is given by the proprieties of the photoresist mask. The ablation threshold of PMMA is 2.6 J/cm^2 at 800 nm wavelength and 150 fs pulse duration [20], much higher compared with silicon, metals or other non-transparent materials. Because numerical simulation shows that the maximum intensification is only a couple of times higher than the incident laser intensity, the PMMA can be used as intensification mask without any risk of damage. The experiment was repeated several times using the same photoresist mask on silicon surface for checking the reliability of the method. No distorted patterns due to the distance variations in the micrometer range between mask and substrate were observed. This remark confirms the assumptions made after numerical simulations that the processing is still feasible even if the mask is not in perfect contact with the target.

5. Conclusions

The presented method is an alternative to conventional processing methods. The optical near-field intensification effect can be used to generate arbitrary patterns by simply controlling the geometry of the mask. In our case, a rectangular-shaped PMMA photoresist mask with 2 μm period was used to create on a silicon surface nanometer-size grooves, in the range of 250 nm width and 15 nm deep. Uniform and continuum nanostructures were imprinted on an area with a diameter of about 100 μm by using a single infrared femtosecond laser pulse. Due to the extended focal region, the planarity control of the mask is not critical in the micrometer range. Also, due to the high ablation threshold of the transparent photoresist mask, it can be used for multiple laser irradiations in applications requiring fast processing on large areas such as microelectronics and plasmonic nanostructures.

Acknowledgments

This work was supported by UEFISCDI under the project DYLIPSS, contract number 7RO-FR/2013.

#200957 - $15.00 USD Received 7 Nov 2013; revised 21 Jan 2014; accepted 21 Jan 2014; published 5 Feb 2014